On the Properties of the $YBa_8Cu_4O_{12+\eta}$ Phase

H. Fjellvåg,[a] P. Karen,[a] A. Kjekshus[a] and J. K. Grepstad[b]

[a]Department of Chemistry, University of Oslo, Blindern, N-0315 Oslo 3 and [b]National Laboratory for Surface Science, Norwegian Institute of Technology, N-7034 Trondheim-NTH, Norway

Fjellvåg, H., Karen, P., Kjekshus, A. and Grepstad, J. K., 1988. On the Properties of the $YBa_8Cu_4O_{12+\eta}$ Phase. – Acta Chem. Scand., Ser. A 42: 171–177.

The properties of the $YBa_8Cu_4O_{12+\eta}$ phase have been studied by powder X-ray and neutron diffraction, magnetometric and core-level photoelectron spectroscopic (XPS) measurements. $YBa_8Cu_4O_{12+\eta}$ exhibits distinctly non-stoichiometric character, where the homogeneity envelope involves the yttrium, copper and oxygen constituents. The formula unit can accommodate an additional amount of 0.3 Y and/or 0.5 Cu for samples fired at 910 °C. The variable oxygen content corresponds to a range of formal oxidation states for Cu of from ~1.8 to at least 2.25. $YBa_8Cu_4O_{12+\eta}$ has a pronounced basicity that makes it sensitive to hydrolysis and high-temperature carbonatization. The (*formally* seen) mixed, high valence state of copper is responsible for the black, metallic appearance of $YBa_8Cu_4O_{12+\eta}$ and its distinct oxidizing properties (e.g., it oxidizes water to O_2). The structural arrangement of $YBa_8Cu_4O_{12+\eta}$ is perovskite-like, but the crystallographic details are not yet fully resolved.

The discovery[1,2] of high-temperature superconductivity with T_C around 90 K for the quaternary phase $YBa_2Cu_3O_{9-\delta}(\delta \approx 2)$ has initiated studies to provide proper characterization of other ternary and quaternary phases in the Y–Ba–Cu–O system. The high-T_C superconductivity in the so-called ceramic oxides is generally connected with phases with structure related to the perovskite type.[3] Scattered reports have appeared in the literature (cf., e.g., Ref. 4) on indications of even higher superconductivity onset temperatures in the Y–Ba–Cu–O system. Reproducibility has been poor, however, and no specific phase relating to these observations has as yet been identified. Such reports, together with the fact that we still lack a clear theoretical picture of the high-T_C superconductivity in these materials, call for a full exploration of the phase diagram and the physical properties of the different phases.

Recently, a yet uncharacterized quaternary phase appearing in the barium-rich corner of the Y–Ba–Cu–O phase diagram has been reported (cf., e.g., Refs. 5–9). Different investigators claim quite different chemical formulae for this phase, as well as different (although related) descriptions of the unit cell. Such discrepancies are probably indicative of rather complicated structural features. In this communication, we discuss the properties of the $YBa_8Cu_4O_{12+\eta}$ phase as inferred from powder diffraction, magnetometric and photoelectron spectroscopic (XPS) measurements.

Experimental

The samples were prepared from Y_2O_3 (Megon, 99.999 %), $BaCO_3$, and CuO or $Cu(OH)_2 \cdot CuCO_3 \cdot xH_2O$ (Merck, reagent grade). Mixtures of dried and analyzed components were homogenized by milling under acetone in a Fritsch Pulverisette laboratory grinder (three ~12 g agate balls) for 12 h. Loosely poured powder beds or lightly pressed pellets were subjected to 2–4 heating sequences (interrupted by intermediate milling under carbon tetrachloride) in corundum boats at 910 °C in air or oxygen (99.8 %; 40 ppm CH_4 impurity) for 24 h, and at 350 °C for 12 h. Reduced oxygen partial pressures were obtained at given temperatures by means of separately placed Cu/Cu_2O "buffers" inside closed silica-glass ampoules (equilibration period: 6 d). The liquid-mix technique[10] was used

to simplify preparation of samples with very small variations in composition without relinquishing the high degree of homogeneity. According to this procedure, Y_2O_3, $BaCO_3$ and $Cu(OH)_2 \cdot CuCO_3 \cdot xH_2O$ were dissolved with stirring in a hot, concentrated solution of (4 mol) citric acid (per 1 mol Y and 1 mol Ba). The clear, blue, viscous solution was subsequently dried to a porous solid. The organic constituent was combusted by heating for 12 h at 850 °C. The pelletized samples were subsequently subjected to two of the additional heating sequences described above. The composition of the samples was checked by chemical analysis: Cu and O were determined iodometrically,[11] Y complexometrically[12] and Ba gravimetrically[5] as $BaSO_4$.

All samples were checked for homogeneity and characterized by the Guinier powder X-ray diffraction technique (Cr$K\alpha_1$ or Cu$K\alpha_1$ radiation). Experimental details concerning the high-temperature powder X-ray diffraction, neutron diffraction, magnetometric and core-level photoelectron spectroscopic (XPS) measurements are described in Refs. 5 and 13.

Results and discussion

The quaternary $YBa_8Cu_4O_{12+\eta}$ phase constitutes a new discovery in the Y–Ba–Cu–O system. A significant feature is the existence of a small, yet distinct homogeneity region with respect to the Y, Cu and O contents. As can be seen from the enlarged portion of the quasi-ternary phase diagram (Fig. 1), the homogeneity region extends from the basic composition $YBa_8Cu_4O_{12+\eta}$ in directions towards the Y- and Cu-rich corners. Note that the formula $YBa_6Cu_3O_{15-\eta}$ used in Ref. 5 refers to a composition included in the homogeneity range of $YBa_8Cu_4O_{12+\eta}$. The neighbouring phases for samples prepared in 1 atm oxygen were Y_2BaCuO_5, $BaCuO_{2+v}$ and $BaCO_3$. Chemical analysis data expressed as metal oxides seem to be some 95 % and hence the presence of carbonate in the $YBa_8Cu_4O_{12+\eta}$ structure cannot be excluded. As is the case for $YBa_2Cu_3O_{9-\delta}$, $YBa_8Cu_4O_{12+\eta}$ exhibits a variable oxygen content depending strongly on the oxygen partial pressure during the final heat treatment of the sample above ~400 °C. For the basic composition, the oxygen content varies from $YBa_8Cu_4O_{14.10\pm0.04}$ for samples prepared in pure oxygen to $YBa_8Cu_4O_{13.02\pm0.04}$ for samples quenched from 750 °C at $p_{O_2} = 2.3 \cdot 10^{-10}$ atm. Clearly, the oxygen content also varies with the location of the sample within the homogeneity region. The amount of oxygen can be stipulated by using a formal copper valence of 2.30 ± 0.02 for pure oxygen conditions and some 2.1 for preparations

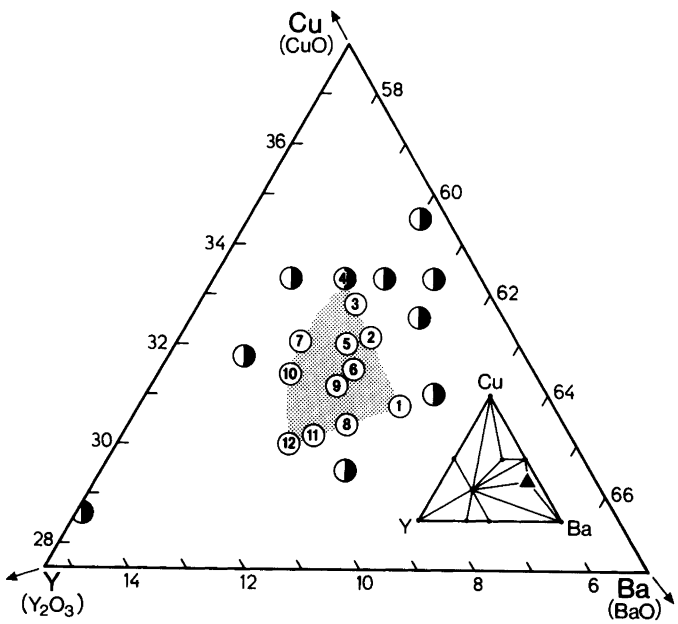

Fig. 1. An enlarged portion of the quaternary phase diagram for the Y–Ba–Cu–O system as projected onto the Y–Ba–Cu plane at 1 atm O_2 and below 910 °C. The inset shows the location of the enlarged portion within the full diagram (reported in Ref. 5). The shaded region depicts the homogeneity region of the $YBa_8Cu_4O_{12+\eta}$ phase with regard to the metal constituents. Open circles refer to single-phase samples; numbers correspond to those in Table 2.

in air. The (*formally* seen) mixed, high valence state of Cu is responsible for the black, metallic appearance of $YBa_8Cu_4O_{12+\eta}$ and its distinct oxidizing properties: e.g., it oxidizes water to O_2 (enhanced by the presence of an acid). The high Ba content gives $YBa_8Cu_4O_{12+\eta}$ a pronounced basicity that makes the samples sensitive to hydrolysis and to high-temperature carbonatization. The phase decomposes above 950 °C.

The powder X-ray diffraction pattern for the $YBa_8Cu_4O_{12+\eta}$ phase changes character when the Y and Cu contents are varied. However, a common feature of the various diffraction diagrams is that all strong reflections can be indexed on the basis of a small, slightly distorted cubic cell ($a \approx$ 404 pm). The intensity distribution of these Bragg reflections clearly suggests a perovskite-like atomic arrangement with Y and Cu atoms in

Table 1. *d*-spacings (in pm) and relative intensities of powder X-ray diffraction reflections for the $YBa_8Cu_4O_{12+\eta}$ phase. Using a cell with doubled perovskite-like dimensions in all (three) directions, the least distorted $YBa_8Cu_4O_{14.1}$ has a = 808.0 ± 0.6 pm, and the distinctly distorted $Y_{1.15}Ba_8Cu_4O_{14.3}$ has a = 805.1 ± 0.1, b = 809.8 ± 0.1, c = 826.0 ± 0.2 pm.

$YBa_8Cu_4O_{14.1}$			$Y_{1.15}Ba_8Cu_4O_{14.3}$	
d	I/I_{max}	*hkl*	*d*	I/I_{max}
801	9	$\frac{1}{2}00$	804	7
		001	413	6
		010	405	6
403	18	100	402.5	6
		101,011	288.8	64
285.6	100	110	285.7	36
233.2	16	111	234.8	16
		$\frac{3}{2}01$	225.0	1.5
224.1	4	$\frac{3}{2}10$	224.0	2
		002	206.7	8
		020	202.4	8
202.0	22	200	201.3	8
196	1	$\frac{3}{2}11$		
		102,012	183.7	3
		021	181.8	1.5
		201,120	180.9	3
180.7	9	210	180.3	1.5
		112	167.4	12
		121	165.6	12
164.9	34	211	165.2	13
150.1	3	$\frac{3}{2}21$	150.6	1
		022	144.5	4
		202	144.1	4
142.8	11	220	142.8	4
		212,122	135.9	3
134.7	4	221	135.0	1.5
		013,103	130.3	3
		031	128.3	2
		130	128.0	2
		301	127.6	2
127.8	11	310	127.5	2
126.1	1	$\frac{3}{2}22,\frac{1}{2}31$		
		113	124.0	0.5
		131	122.2	0.5
121.7	3	311	121.7	0.5
116.6	3	222	117.4	3

octahedral sites. The additional reflections call for a larger superstructure cell, and line-splittings show that the symmetry is lower than cubic.

Assuming a proper (cubic, $a_p = a$) perovskite-type structure with barium at the origin of, and oxygens (the number of which is virtually unimportant) at their appropriate sites in, the unit cell, the average scattering power (electron content) at the ½, ½, ½ position was estimated[14] by comparison of observed and calculated integrated intensities of the powder diffraction patterns. The result gave 19–21 electrons at ½, ½, ½ per (assumed) perovskite-type unit cell, thus demonstrating that this site of the sub-cell is occupied by yttrium, copper and vacancies. Estimates of the unit cell content based on pycnometric densities are necessarily burdened with some uncertainty (originating from the density measurements as well as from ambiguity concerning the true unit cell), but confirm beyond doubt that the $YBa_8Cu_4O_{12+\eta}$ atomic arrangement comprises appreciable vacancies when compared with an ideal perovskite-type structure. The same inference is also obtained on comparing added volume increments with the "observed" volume of the sub-cell ($57.4 \cdot 10^6$ versus $66.2 \cdot 10^6$ pm^3, respectively). With this as background, and, moreover, to provide a convenient starting point for describing the variable composition within the homogeneity range, the formula $Ba(Cu_{4/8}Y_{1/8}\square_{3/8})O_{3-x}$ is adopted to specify the content of the sub-cell (where □ denotes vacancy).

Since neither the size nor the symmetry of the superstructure of the $YBa_8Cu_4O_{12+\eta}$ phase is ascertained, it is convenient to relate the following considerations to the perovskite-like sub-cell. The analytical formula $YBa_8Cu_4O_{12+\eta}$ can, e.g., be arrived at by doubling of the sub-cell in all (three) directions, but the diffraction patterns can in reality be satisfactorily indexed on the basis of various smaller, tetragonal unit cells. In fact, quite satisfactory agreement between observed and calculated intensities can be obtained for several structural models, but the present data do not allow a choice between these. To approach the true structure of $YBa_8Cu_4O_{12+\eta}$ more closely, the unit cell and space group ought to be established by application of single-crystal or electron microscopy methods.

The possibility of variously filled and variously ordered vacancies both in the cation (*vide supra*) and anion (some 40 % vacancies compared with the ideal perovskite-type atomic arrangement)

Table 2. Unit cell dimensions (in pm) for various compositions from the homogeneity envelope of the $YBa_8Cu_4O_{12+\eta}$ phase. Numbers correspond to those in Fig. 1. Inaccuracies do not exceed one unit in last digit. Deviation limits (in pm) a: ±1, b: ±2, c: ±3, d: ±4, e: ±5 for *c* express broadening of appropriate reflections, based on the range in which ~90 % of the whole intensity occurs.

Analytical formula	*a*	*b*	*c*	No.
$YBa_8Cu_4O_{13.90}$	404.0[a]			1
$YBa_8Cu_4O_{13.75}$	404.4[a]			1
$YBa_8Cu_4O_{13.15}$	402.6	405.1	409;b	1
$YBa_8Cu_{4.25}O_{14.30}$	403.3	405.2	406;b	2
$YBa_8Cu_{4.40}O_{14.46}$	403.7	405.4	408;b	3
$YBa_8Cu_{4.5}O_{14.59}$	403.9	405.7	409;b	4
$Y_{1.06}Ba_8Cu_{4.27}O_{14.40}$	403.3	405.0	409;c	5
$Y_{1.06}Ba_8Cu_{4.27}O_{14.14}$	403	406	409;c	5
$Y_{1.08}Ba_8Cu_{4.17}O_{14.32}$	403.1	406	409;c	6
$Y_{1.08}Ba_8Cu_{4.17}O_{13.16}$	402.6	404.6	411;a	6
$Y_{1.17}Ba_8Cu_{4.33}O_{14.82}$	403.8	404.4	412;c	7
$Y_{1.15}Ba_8Cu_4O_{14.24}$	402.5	404.9	413;b	8
$Y_{1.15}Ba_8Cu_{4.15}O_{14.50}$	402.6	404.7	412;c	9
$Y_{1.25}Ba_8Cu_{4.25}O_{14.65}$	402.6	405.0	413;e	10
$Y_{1.25}Ba_8Cu_4O_{14.32}$	403.2	404.4	414;d	11
$Y_{1.33}Ba_8Cu_4O_{14.62}$	402.8	406	414;d	12

[a]Close inspection of reflection profiles indicates slight distortion from cubic symmetry.

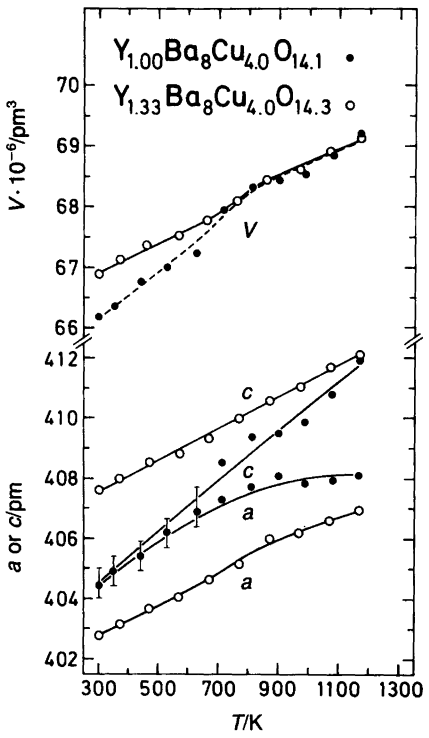

Fig. 2. Variation of unit cell dimensions (of perovskite-like sub-cell; see text) with temperature between 300 and 1200 K for $Y_{1.33}Ba_8Cu_{4.0}O_{14.3}$ and $Y_{1.00}Ba_8Cu_{4.0}O_{14.1}$ (using tetragonal and cubic approximation, respectively, due to the diffuse broadening of reflections; see text).

sub-lattices gives ample opportunities for distortion from the cubic symmetry of the basic perovskite-type lattice. The prototype composition $YBa_8Cu_4O_{12+\eta}$ adopts the least distorted structure, and is very nearly cubic (cf. Tables 1 and 2). A splitting of the reflections for the more yttrium- and copper-rich samples can be accounted for in terms of orthorhombic symmetry, as demonstrated in Table 1 for the $Y_{1.15}Ba_8Cu_4O_{14.3}$ sample. Filling of the vacancies which occur in the structure at the prototype composition with yttrium and/or copper (*vide supra*, cf. samples Nos. 2–4, 8, 11 and 12 in Fig. 1 and Table 2) increases the unit cell dimensions as well as the orthorhombic distortion (the latter feature is most prominent in the direction denoted *c*, where $(c-a)/a$ amounts to ~0.025 for the most Y-rich samples). A certain disorder also clearly occurs in the *c* direction, manifesting itself as broadening of the reflections denoted 00*l* and *hhl* in Table 1. The most pronounced disorder of this kind is found for the most yttrium- *and* copper-rich samples. In addition to the structural distortions brought about by the short-range order of Y, Cu and vacancies, the amount of O and its distribution among the different oxygen sites greatly influences the $YBa_8Cu_4O_{12+\eta}$ structure. Generally, the unit cell dimensions and the lattice distortion increase with increasing oxygen content.

The sparse structural information[6–8] on the $YBa_8Cu_4O_{12+\eta}$ phase in the current literature sketches a picture in accordance with the above description.

The variation of the unit cell dimensions with temperature is shown in Fig. 2 for the least and the most distorted $YBa_8Cu_4O_{12+\eta}$ structures with analytical formulae $Y_{1.00}Ba_8Cu_{4.0}O_{14.1}$ and $Y_{1.33}Ba_8Cu_{4.0}O_{14.3}$, respectively. The only slight distortion for the former composition increases distinctly with temperature. No indications of any phase transitions are found. The average, linear thermal expansion coefficient for the entire temperature range 300–1300 K is $\alpha_V \approx 3.5 \cdot 10^{-5}$ K^{-1}, which is virtually the same as that found for Y_2BaCuO_5 and A-type $YBa_2Cu_3O_{9-\delta}$.[5] The continuous, transition-like increase in the slope of the $V(T)$ curve for $Y_{1.33}Ba_8Cu_{4.0}O_{14.3}$ (Fig. 2) in the range 600–900 K is probably related to an oxygen loss which results in increased unit cell volume, the behaviour being quite analogous to that of $YBa_2Cu_3O_{9-\delta}$ $(2<\delta<3)$.[5] Based on this analogy, one arrives at a reduction in oxygen content of some 5 % for $Y_{1.33}Ba_8Cu_{4.0}O_{14.3}$ in the conversional region.

The recorded XPS core-level spectra of $Y_{1.33}Ba_8Cu_{4.0}O_{14.3}$ exhibit resemblances to those of Y_2BaCuO_5 and $YBa_2Cu_3O_{9-\delta}$.[13,15,16] The spectra of the cold-pressed sample (with no further *in situ* surface preparation) disclose the presence of significant amounts of surface carbonate, identified by its C 1*s* spectrum. In addition to the peak at 285.0 eV binding energy, which is attributed to hydrocarbon contamination, a second feature is observed at 289.6 eV. This highly oxidized surface carbon has also been found in previous photoemission studies of the superconducting $YBa_2Cu_3O_{9-\delta}$ phase[13,17,18] and was attributed to $BaCO_3$ on the surface.

This assignment is corroborated by the recorded peak intensities and the measured binding energies of the predominant features of the O 1*s*

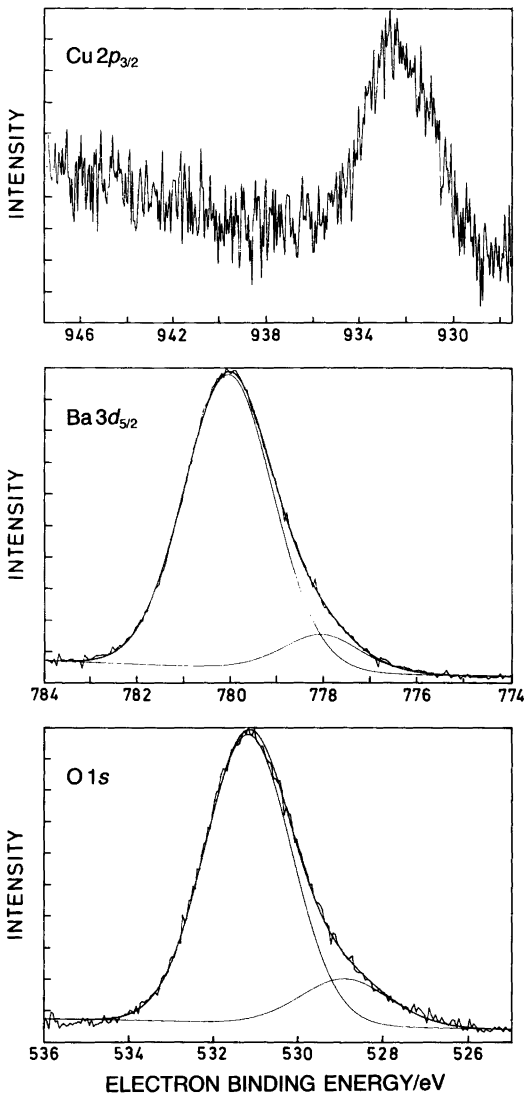

Fig. 3. XPS core-level spectra (Cu $2p_{3/2}$, Ba $3d_{5/2}$ and O 1*s*) of $Y_{1.33}Ba_8Cu_{4.0}O_{14.3}$.

(531.2 eV) and Ba $3d_{5/2}$ (780.0 eV) spectra (see Fig. 3). A superposition of two chemically shifted peaks is invariably reported for the oxygen and barium core levels in XPS studies of the superconducting $YBa_2Cu_3O_{9-\delta}$ phase[13,15,18] and Ba-doped La_2CuO_4.[19] In a combined SEM and photoemission study of $YBa_2Cu_3O_{9-\delta}$, Schrott *et al.*[18] – exploring different methods for *"in situ"* surface preparation – report that the high binding-energy features of the O 1*s* and Ba 4*d* spectra increase in intensity (the O 1*s* feature scaling almost linearly) with the amount of surface carbonate (as determined from the C 1*s* peak at ~289 eV). Their relative emission intensities are also observed to increase (at the expense of the low binding-energy features) for spectra recorded with boosted surface sensitivity, i.e. using high electron-escape angles[19] or synchrotron radiation tuned to minimize the mean free path of the photoelectrons.[18]

The possibility of a $BaCO_3$ surface impurity was not considered by Steiner *et al.*,[15,19] who attribute the double peak structure of the Ba $3d_{5/2}$ spectrum to the existence of oxygen defects in neighbouring sites. Instead, they ascribed the O 1*s* double peak tentatively to O^- ions, CO or CO_2 adsorbed on the sample surface.

In the study of Schrott *et al.*,[18] $BaCO_3$ contamination was found also for samples prepared using BaO as a starting material. Furthermore, it was observed that the amount of $BaCO_3$ depended on the temperature used for the final O_2 annealing. Accordingly, unreacted $BaCO_3$ starting material cannot be the source of this surface impurity, which they suggest is formed by reaction with residual CO_2 in the annealing atmosphere.

We propose the same origin for the $BaCO_3$ surface contamination observed in this study. From the chemistry of the sample syntheses, surface or grain-boundary segregation of unreacted $BaCO_3$ appears most unlikely. Furthermore, an inherent instability of this phase with respect to formation of $BaCO_3$ is detectable, a behaviour quite analogous to that of $YBa_2Cu_3O_{9-\delta}$.[11]

The XPS binding energy of the Y $3d_{5/2}$ level of $Y_{1.33}Ba_8Cu_{4.0}O_{14.3}$ was determined as 156.7 ± 0.2 eV, which is slightly higher than observed for Y_2BaCuO_5 and $YBa_2Cu_3O_{9-\delta}$.[13,15,20] The recorded Cu $2p_{3/2}$ spectra, however, differ from those observed for Y_2BaCuO_5 and $YBa_2Cu_3O_{9-\delta}$. The Cu $2p_{3/2}$ spectrum of $Y_{1.33}Ba_8Cu_{4.0}O_{14.3}$ (Fig. 3) shows no satellite structure ~10 eV above the main peak, characteristic of the "poorly screened" Cu $2p^53d^9$ final state associated with a Cu^{2+} ground state.[13,15,16,20–22] Furthermore, we observe a pronounced change in the Cu $2p_{3/2}$ line shape and a chemical shift of about 0.7 eV to lower binding energy compared to the (orthorhombic) $YBa_2Cu_3O_{9-\delta}$ phase. This shift, together with the absence of shake-up satellites, indicates a monovalent Cu ground state with a filled 3*d* shell

($3d^{10}$). The spectrum resembles that of Cu_2O and can probably be explained by surface decomposition of the highly oxidized copper in $Y_{1.33}Ba_8Cu_{4.0}O_{14.3}$. Such decomposition has previously been reported for CuO when sputter-cleaned[23] or heated above 250 °C in vacuum.[24] Occasionally, it has also been observed in XPS of non-treated[22] and sputter-cleaned[25] $YBa_2Cu_3O_{9-\delta}$ surfaces.

The magnetometric measurements suggest that also the $YBa_8Cu_4O_{12+\eta}$ phase exhibits superconducting properties with weak, almost temperature-independent paramagnetism above about 70 K. However, this aspect will be discussed in more detail in a forthcoming paper.[26]

The $YBa_8Cu_4O_{12+\eta}$ phase of the Y–Ba–Cu–O system has counterparts in systems where e.g. Sc and Lu have replaced Y.[25] However, in the corresponding systems with rare earths of larger ionic radius (e.g. Nd^{3+}) such a phase does not exist,[26] nor does it form when Sr replaces Ba.[26] We intend to report in detail on the crystal structure of this group of phases in a forthcoming publication.[26]

Acknowledgement. This work has received financial support from the Royal Norwegian Council for Scientific and Industrial Research.

References

1. Wu, M. K., Ashburn, J. R., Torng, C. J., Hor, P. H., Meng, R. L., Gao, L., Huang, Z. J., Wang, Y. Q. and Chu, C. W. *Phys. Rev. Lett. 58* (1987) 908.
2. Cava, R. J., Batlogg, B., van Dover, R. B., Murphy, D. W., Sunshine, S., Siegrist, T., Remeika, J. P., Rietman, E. A., Zahurak, S. and Espinosa, G. P. *Phys. Rev. Lett. 58* (1987) 1676.
3. Cava, R. J. In: *Proceedings of the European Workshop on High T_C Superconductors and Potential Applications,* Genova 1987, p. 233.
4. Caplin, D. *Nature (London) 328* (1987) 376.
5. Fjellvåg, H., Karen, P. and Kjekshus, A. *Acta Chem. Scand., Ser. A 41* (1987) 283.
6. Abbattista, F., Vallino, M., Mazza, M., Brovetto, P. and Delunas, A. In: *Proceedings of the European Workshop on High T_C Superconductors and Potential Applications,* Genova 1987, p. 279.
7. Frase, K. G., Liniger, E. G. and Clarke, D. R. *J. Am. Chem. Soc. 70* (1987) C 204.
8. Nakada, I., Sato, S., Oda, Y. and Kohara, T. *Jpn. J. Appl. Phys. 26* (1987) L 697.
9. Roth, R. S., Dennis, J. R. and Davis, K. L. *Adv. Ceram. Mater. 2* (1987) 203.
10. Eror, N. G. and Loehr, T. M. *J. Solid State Chem. 12* (1975) 319.
11. Fjellvåg, H., Karen, P., Kjekshus, A., Kofstad, P. and Norby, T. *Acta Chem. Scand., Ser. A 42* (1988) 178.
12. Körbl, J. and Pribyl, R. *Chem. Anal. 45* (1956) 102.
13. Fjellvåg, H., Karen, P., Kjekshus, A. and Grepstad, J. K. *Solid State Commun. 64* (1987) 917.
14. Capkova, P., Karen, P. and Dobiasova, L. *Cryst. Res. Technol. 21* (1986) 735.
15. Steiner, P., Kinsinger, V., Sander, I., Siegwart, B., Hüfner, S. and Politis, C. *Z. Phys. B 67* (1987) 19.
16. Bianconi, A., Castellano, A. C., De Santis, M., Delogu, P., Gargano, A. and Giorgi, R. *Solid State Commun. 63* (1987) 1135.
17. Yarmoff, J. A., Clarke, D. R., Drube, N., Karlsson, U. O., Taleb-Ibrahimi, A. and Himpsel, F. J. *Phys. Rev. B 36* (1987) 3967.
18. Schrott, A. G., Cohen, S. L., Dinger, T. R., Himpsel, F. J., Yarmoff, J. A., Frase, K. G., Park, S. I. and Purtell, R. *Paper presented at the 34th National AVS Symposium,* Anaheim 1987.
19. Steiner, P., Courths, R., Kinsinger, V., Sander, I., Siegwart, B. and Hüfner, S. *Appl. Phys. A 44* (1987) 75.
20. Dauth, B., Kachel, T., Sen, P., Fischer, K. and Campagna, M. *Z. Phys. B 68* (1987) 407.
21. Fujimori, A., Takayama-Muromachi, E., Uchida, Y. and Okai, B. *Phys. Rev. B 35* (1987) 8814.
22. Horn, S., Cai, J., Shaheen, S. A., Jeon, Y., Croft, M., Chang, C. L. and den Boer, M. L. *Phys. Rev. B 36* (1987) 3895.
23. Panzner, G., Egert, B. and Schmidt, H. P. *Surf. Sci. 151* (1985) 400.
24. Larson, P. E. *J. Electron Spectrosc. Relat. Phenom. 4* (1979) 213.
25. Stucki, A. *Private communication.*
26. Fjellvåg, H., Karen, P. and Kjekshus, A. *To be published.*

Received December 21, 1987.